The Journal of Antibiotics (2017) 70, 981–986

www.nature.com/ja

ORIGINAL ARTICLE

F-36316 A and B, novel vasoactive compounds, isolated from *Incrucipulum* sp. SANK 10414

Yuki Hirota-Takahata[1], Yoko Ishimoto[2], Emi Kurosawa[1], Yuko Iwadate[1], Yoshiko Onozawa[2], Isshin Tanaka[1], Masahiro Tanaka[1] and Hideki Kobayashi[2]

In the course of our screening program for vasoactive compounds using co-culture assay of endothelial cells and fibroblast cells, potent activity was detected in the cultured broth of *Incrucipulum* sp. SANK 10414. Two active compounds, F-36316 A and B, and a non-active homolog, F-36316 C, were isolated from the broth. The structures of F-36316 A, B and C were elucidated by physicochemical data and spectral analyses, and found to be new 3-acylated tetronic acid homologs. F-36316 A and B induced morphological changes of endothelial cells different from vascular endothelial growth factor (VEGF) or vestaines in the assay with EC_{50} values of 1.8 and 11.7 μM, respectively. Furthermore, F-36316 A and B suppressed VEGF-induced vascular permeability induction in mice.
The Journal of Antibiotics (2017) **70,** 981–986; doi:10.1038/ja.2017.84; published online 9 August 2017

INTRODUCTION

Blood vessels are formed by the proliferation and migration of endothelial cells into extracellular matrix and then newly formed vessel structure is stabilized by coverage with mural cells. This process of angiogenesis and vessel stabilization is regulated in a tight and timely manner by the coordinate effects of various vasoactive factors. Vascular endothelial growth factor (VEGF) is one of the key molecules in angiogenesis and it also regulates vascular permeability.[1] Although VEGF has a critical role in new vessel formation, overproduction of VEGF leads to formation of fragile vessels that are not stabilized properly and lack enough function to supply oxygen and nutrients; this is one of the key causes of some human diseases, such as diabetic retinopathy and moyamoya disease.[2–5] Therefore, a compound able to eliminate fragile vessels by adequately suppressing excess angiogenesis or enhancing vessel stabilization would be useful for treating these clinical conditions.

In our previous reports, we had established an assay system named VS-G assay for screening of vasoactive compounds based on morphological changes of endothelial cells,[6] and through the course of the screening campaign of a natural product library by using the VS-G assay, we discovered vestaines, which have the unique property of being both pro-angiogenicity and anti-permeability.[6,7] By the subsequent search for substances with an activity to induce morphological changes of cells different from that of VEGF and vestaines, this characteristic activity was found in the cultured broth of the fungus named *Incrucipulum* sp. SANK 10414, and following isolation studies revealed two novel compounds, F-36316 A and B (Figure 1).

In this report, we describe the screening, taxonomy of the producing organism, isolation, physicochemical properties, structural elucidations and biological activities of F-36316s.

RESULTS

Screening of vasoactive compounds

Screening was carried out by using the VS-G assay.[6] Among 13 000 cultured broths of microorganisms, a fungus strain SANK 10414 was found to cause a morphological change to the cells different from that of VEGF and vestaines.

Taxonomy of the producing organism

The phylogenetic tree using ITS-5.8S rDNA sequences is shown in Figure 2. Phylogenetic analysis revealed that the strain SANK 10414 belongs to the clade of the genus *Incrucipulum*. Thus, the strain SANK 10414 was identified as *Incrucipulum* sp. SANK 10414.

Isolation

Isolation was done in several lots. Representative isolation methods are described as follows. The cultured broth (1 liter) was centrifuged and separated into mycelium and supernatant. The active substances were extracted from the mycelium with acetone (400 ml) and centrifuged to obtain the supernatant. The supernatant was concentrated *in vacuo* to remove acetone. After the pH of the concentrate was adjusted to 3.0 with 1 N HCl, active compounds were extracted with ethyl acetate (125 ml). The organic layer was washed with brine, dried over anhydr. Na_2SO_4 and concentrated *in vacuo* to give an oily substance (96.8 mg). The substance was purified by preparative HPLC using an ODS column (SYMMETRY C18, 19 i.d. × 100 mm, Waters, Milford, MA,

[1]Organic Synthesis Department, Daiichi Sankyo RD Novare Co., Ltd, Tokyo, Japan and [2]Frontier Research Laboratories, Daiichi Sankyo Co., Ltd, Tokyo, Japan
Correspondence: Dr H Kobayashi, Frontier Research Laboratories, Group I, Daiichi Sankyo Co. Ltd, 1-2-58 Hiromachi, Shinagawa-ku, Tokyo 140-8710, Japan.
E-mail: kobayashi.hideki.gc@daiichisankyo.co.jp
Received 29 April 2017; revised 27 June 2017; accepted 27 June 2017; published online 9 August 2017

USA). The chromatography was performed with MeCN/10 mM aq. Na_2SO_4 in 0.03% phosphoric acid (58:42) at a flow rate of 5 ml min^{-1}.

*Isolation of F-36316 A (**1**).* Compound **1** was eluted from 14.2 to 17.0 min in the preparative HPLC as described above. For desalting, the eluate was concentrated *in vacuo* to remove MeCN and then was subjected to a SP207 column (Mitsubishi Chemical, Tokyo, Japan, 5 ml). After washing the column with water (20 ml), **1** was eluted with 80% aq. acetone (20 ml). The eluate was concentrated to dryness to give **1** as a white powder (6.2 mg).

*Isolation of F-36316 B (**2**).* Compound **2** was eluted from 8.5 to 11.5 min in the preparative HPLC as described above. The eluate was desalted in the same manner as **1** and concentrated to dryness to give **2** as a white powder (18.3 mg).

*Isolation of F-36316 C (**3**).* Compound **3** was eluted from 6.0 to 7.5 min in the preparative HPLC described above. The eluate was desalted in the same manner as **1** and concentrated to dryness to give a partially purified substance (8.3 mg). The substance was re-chromatographed by the same preparative HPLC using the solvent system of MeCN/0.1 M aq. $NaClO_4$ (51:49) at a flow rate of 5 ml min^{-1}, desalted in the same manner as **1** and concentrated to dryness to give **3** as a white powder (5.0 mg).

Physicochemical properties

Physicochemical properties of F-36316s are summarized in Table 1. As sodium was observed in the elemental analysis, F-36316s were seemed to have the property of chelating metal ions.

Structural elucidation

*Structural elucidation of F-36316 A (**1**).* The structural elucidation was mainly focused on **1**. The molecular formula of **1** was determined as $C_{20}H_{32}O_7$ by the negative ion mode ESI–HR–MS. The degree of unsaturation calculated by this molecular formula was five.

The ^1H and ^{13}C NMR spectral data of **1** obtained in dimethylsulfoxide-d_6 are summarized in Table 2. Although **1** showed a pair of the signals just after being dissolved, these signals converged at the center of each signal over time. Therefore, **1** seemed to have a tautomerism.

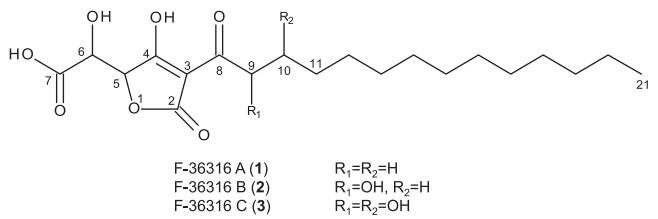

Figure 1 Structures of F-36316s.

The structural elucidation was carried out to use the converged signals. In the ^1H NMR spectrum of **1**, signals of the highly overlapped alkyl group (δ 1.20–1.30), one methyl, two methylene and two methine signals were observed. In the ^{13}C NMR spectrum, 11 assignable carbon signals were observed and classified into 1× methyl, 3× methylene, 2× methine and five quaternary carbons, as well as complexly overlapped methylene carbon signals in the alkyl region. In addition, three characteristic carbon signals, C-3 (δ 96.0), C-5 (δ 80.5) and C-6 (δ 70.4) were observed. According to the DEPT spectra, one methylene signal (C-9) was recognized to be overlapped with the solvent signals.

The partial structures elucidated by several NMR techniques such as double quantum filtered COSY (DQF-COSY), HSQC, HMBC and incredible natural abundance double quantum transfer experiment (INADEQUATE) are shown in Figure 3. In the INADEQUATE spectrum, the correlations from C-4 to C-7 were observed. Although the correlation between H-5 and C-3 was not observed in the HMBC spectrum, that between H-6 and C-3 was observed weakly. Therefore, as well as the correlations from H-9 to C-3 and C-8, it was considered that C-4 was connected to C-3, namely C-3 was located between C-4 and C-8. This hypothesis was also supported by their chemical shifts. The chemical shifts of C-4 (δ 192.2) and C-8 (δ 193.7) were rather high as a carbonyl carbon, and that of C-3 (δ 96.0) was also high as an olefinic carbon. These results were consistent with the existence of an enol or an enone.

In the case of C-2, the signal at δ 174.5 was regarded as a carbonyl of an ester group. Based on the observed C-H long-range correlation between H-5 and C-2 and the chemical shift of C-5 (δ 80.5), the partial structure of 2-furanone was derived. Thereby, the alkyl chain from C-9 was axiomatically determined. Thus, the structure of **1** was determined to be a new 3-acylated tetronic acid homolog as shown in Figure 1. The observed tautomerism of **1** was proved to be occurring at the tetronic acid moiety[8] and four assumed tautomers are shown in Figure 4.

The ^1H, ^{13}C, DQF-COSY, HSQC, HMBC, INADEQUATE and NOESY spectra of **1** are presented in the Supplementary Information.

Structural elucidation of other homologs. The structural elucidations of the homologs **2** and **3** were carried out in the same way as **1**. Although **2** and **3** did not show a pair of signals originated from the expected tautomers that were the same as **1**, the signals of the tetronic acid moieties were broadened.

The structural differences of **2** and **3** compared with **1** originated from the substituent pattern of the hydroxyl group at C-9 or C-10. By mass spectral analysis and NMR spectral analysis, the structures of **2** and **3** were elucidated as the 9-hydroxylated derivative and the 9, 10-dihydroxylated derivative of **1**, respectively (Figure 1).

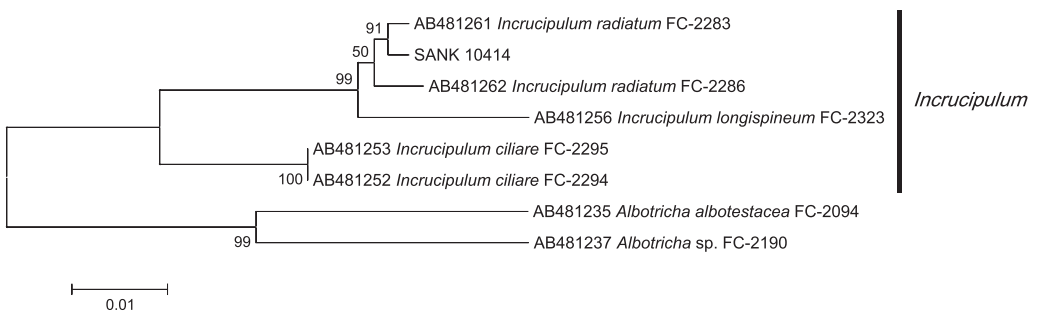

Figure 2 The taxonomic position of the strain SANK 10414. Bootstrap values (%) are indicated at the branches from 1000 replications. The scale bar below the phylogenetic tree indicates substitution per site.

Table 1 Physicochemical properties of F-36316 A, B and C

	*F-36316 A (**1**)*	*F-36316 B (**2**)*	*F-36316 C (**3**)*
Appearance	White powder	White powder	White powder
HR-MS (m/z)			
Found:	383.2075 $(M-H)^-$	399.2020 $(M-H)^-$	415.1968 $(M-H)^-$
Calcd.:	383.2064 (for $C_{20}H_{31}O_7$)	399.2013 (for $C_{20}H_{31}O_8$)	415.1962 (for $C_{20}H_{31}O_9$)
$[\alpha]_D^{25}$ (c 0.50, 50% EtOH)	−75.8°	−78.4°	−84.4°
UV $\lambda_{max}^{50\%\ EtOH}$ nm (ε)	266 (16 000), 233 (14 000)	268 (16 000), 233 (14 000)	268 (15 000), 233 (14 000)
IR ν_{max} cm^{-1} (ATR)	3575, 3217, 2918, 2850, 1703, 1597, 1466	3388, 2920, 2852, 1722, 1622, 1566, 1460	3359, 2919, 2850, 1726, 1648, 1563, 1461

Table 2 ^1H and ^{13}C NMR signal assignments of F-36316s in DMSO-d6

	*F-36316 A (**1**)*[a]		*F-36316 B (**2**)*		*F-36316 C (**3**)*	
Position	δ_C	δ_H	δ_C	δ_H	δ_C	δ_H
2	174.5 (s)		174.0 (s)		174.1 (s)	
3	96.0 (s)		94.0 (s)		94.2 (s)	
4	192.2 (s)		192.4 (s)		192.3 (s)	
5	80.5 (d)	4.38 (1H, d, 2.2 Hz)	81.1 (d)	4.44 (1H, d, 2.2 Hz)	81.0 (d)	4.44 (1H, d, 2.2 Hz)
6	70.4 (d)	4.20 (1H, d, 2.2 Hz)	70.2 (d)	4.26 (1H, d, 2.2 Hz)	70.0 (d)	4.29 (1H, d, 2.2 Hz)
7	172.0 (s)		171.8 (s)		171.7 (s)	
8	193.7 (s)		194.3 (s)		192.7 (s)	
9	39.4[b] (t)	2.58 (2H, m)	73.3 (d)	4.38 (1H, m)	75.2 (d)	4.49 (1H, br.)
10	24.5 (t)	1.42 (2H, m)	34.2 (t)	1.21 (1H, [c])	71.0 (d)	3.67 (1H, m)
				1.58 (1H, m)		
11	28.6-29.1 (t)	1.20-1.30 (20H, [b])	25.3 (t)	1.32 (2H, m)	34.2 (t)	1.42 (2H, m)
12	(t)		28.6-29.1 (t)	1.15-1.30 (18H, [c])	25.4 (t)	1.20-1.30 (18H, [c])
13	(t)		(t)		28.6-29.2 (t)	
14	(t)		(t)		(t)	
15	(t)		(t)		(t)	
16	(t)		(t)		(t)	
17	(t)		(t)		(t)	
18	(t)		(t)		(t)	
19	31.2 (t)		31.2 (t)		31.2 (t)	
20	22.0 (t)		22.0 (t)		22.0 (t)	
21	13.8 (q)	0.85 (3H, t, 7.0 Hz)	13.9 (q)	0.85 (3H, t, 7.2 Hz)	13.9 (q)	0.86 (3H, t, 7.0 Hz)

Chemical shifts are given in ppm referenced to TMS.
[a]The signals were measured 10 days after dissolved.
[b]The signal was measured by DEPT135 spectrum, because it was not clearly observed due to overlap with DMSO signals in ^{13}C NMR spectrum.
[c]Not clearly observed due to overlap.

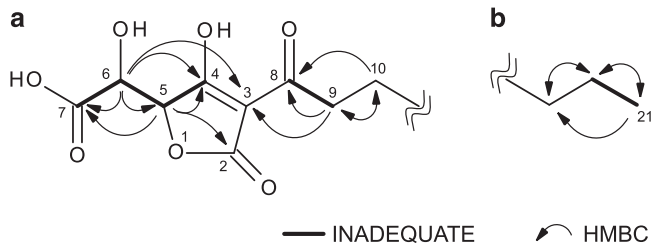

Figure 3 Partial structures (**a**) and (**b**) obtained from the NMR analysis of **1**.

The ^1H and ^{13}C NMR spectra of **2** and **3** are presented in the Supplementary Information.

Biological activities

In vitro activity and its effect on HUVEC morphology in the VS-G assay. In the VS-G assay, green fluorescent protein (GFP)-labeled human umbilical vein endothelial cells (HUVECs) were cultured on human dermal fibroblast feeder cells, and cultured with test compounds for 3 days. At the end of the co-culture, the morphology of the GFP-HUVECs was observed under fluorescent microscopy. VEGF induced a tube-like network of GFP-HUVECs, whereas vestaine A_1 induced an island-shaped pattern (Figure 5a). F-36316 A induced morphological changes of GFP-HUVECs in a different pattern from VEGF or vestaines (Figure 5a). The activities of F-36316s were evaluated based on the area of GFP-HUVECs using the maximum area value treatment with vestaine A_1 as 100 percent activity. As results, F-36316 A and B dose dependently showed activity with EC_{50} values of 1.8 and 11.7 μM, respectively, whereas F-36316 C did not show such activity (Figure 5b).

In vivo vascular leakage assay. To further elucidate the biological effects of F-36316s, the effects on vascular permeability were evaluated in mice. After the intraperitoneal injection of F-36316 A or F-36316 B for 4 h, vascular leakage was induced by the injection of VEGF (60 ng per ear) into the ears of mice and the amount of Evans Blue was

determined as an indicator of vessel permeability. As shown in Figure 6, both F-36316 A and F-36316 B at 10 mg kg^{-1} (i.p.) suppressed the VEGF-induced leakage of Evans Blue dye by ~50%.

DISCUSSION

In the course of our screening program for vasoactive compounds, F-36316 A and B, and non-active compound, F-36316 C, were isolated from the cultured broth of *Incrucipulum* sp. SANK 10414. Structures of the F-36316s were proven to be new 3-acylated tetronic acid homologs. The structural difference among the F-36316s was the number of hydroxyl groups in the alkyl chain. It is interesting that both bacteria and fungi produce such compounds having 3-acylated tetronic acid moieties.[9–12] In addition, it is a remarkable point that they have been reported as antibiotic agents, enzyme inhibitors, metal chelators and so on.[9–15] In this study, we newly found that F-36316 A and B that are 3-acylated tetronic acid homologs, showed the potent activities of both being pro-angiogenicity and anti-permeability *in vitro* and *in vivo*.

In the screening program using the VS-G assay, we had previously obtained vestaines.[7] Although both F-36316 A and vestaines have common structural characteristics, such as having an amphiphilic feature and keto-enol equilibrium, vestaines induced an island-shape morphology in HUVECs, whereas F-36316 A induced mixed forms of islands and tubes (Figure 5a). As the differences in morphology induced by vestaines and F-36316 A were reproduced in many independent VS-G assays, the inducing mechanisms of vestaines and F-36316 A would seem to be different.

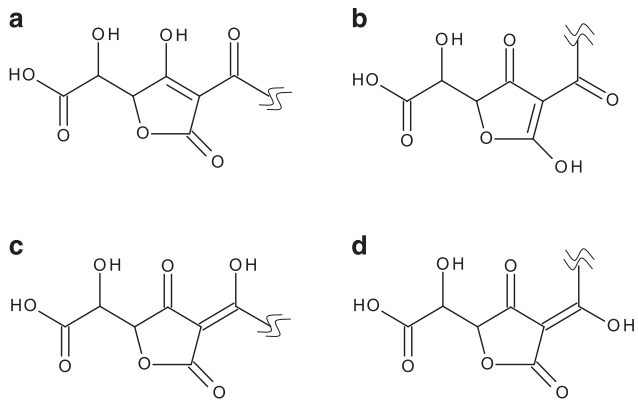

Figure 4 Four assumed tautomers of **1**. Structures of (**a**) and (**b**) are endo-enol types, whereas those of (**c**) and (**d**) are exo-enol types.

As for the mechanism of F-36316 A, we found the following two possibilities according to its structural features. One possibility is that F-36316 A might be able to act as a protein tyrosine phosphatase (PTP) inhibitor. Among known natural products, the structure of F-36316 A resembles RK-682, which was found as an inhibitor of HIV-1 protease,[9,10] and later was reported to inhibit PTPs.[14] Among the PTPs participating in the vessel maturation, vascular endothelial-PTP, which is a receptor type PTP, is specifically expressed in endothelial cells. Inhibition of vascular endothelial-PTP activates Tie2 receptors, and leads to stabilization of the blood vessels.[16,17] RK-682 was reported to inhibit cluster of differentiation 45 (CD45), which is a receptor type PTP, with IC_{50} of 54 μM and vaccinia virus VH1-related phosphatase, which is a cytoplasmic PTP, with IC_{50} of 2 μM.[14] Although there is no report that RK-682 inhibits vascular endothelial-PTPs, F-36316A has the possibility of inhibiting vascular endothelial-PTPs because of the structural similarity.

Another possibility is that F-36316 A might be able to act as a sphingosine-1-phosphate (S1P) receptor 1 agonist. F-36316 A has an amphiphilic feature as does S1P, which is a metabolite of the sphingolipid. S1P causes cell proliferation, cell migrations and so on by binding to the G protein-coupled receptors, S1P receptors.[18,19] $S1P_1$ is one of the receptors of S1P and it is particularly known to have a role of promoting angiogenesis and enhancing vascular stabilization.[20] These actions on vessels are induced by the binding of S1P to $S1P_1$ receptors, but not by the binding of sphingosine before phosphorylation. The phosphate group is necessary to induce these actions. However, F-36316 A has no phosphate groups. According to the reported binding model of RK-682 to VH1-related phosphatase, it was suggested that the acylated tetronic anion is a mimic of the

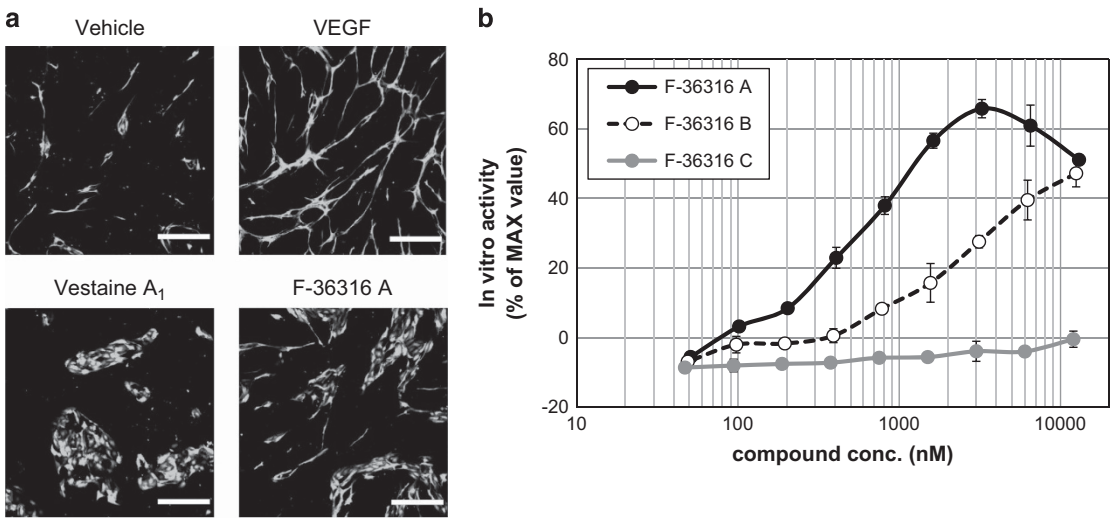

Figure 5 The activity of F-36316s in VS-G assay. (**a**) Morphologies of GFP-HUVECs treated with 0.25% DMSO, VEGF (50 ng ml^{-1}), vestaine A_1 (0.21 μM), or F-36316 A (3.0 μM). The data of vestaine A_1 is representative data obtained by another independent experiment. Each scale bar is 400 μm. (**b**) GFPHUVECs were treated at various concentrations of F-36316s. *In vitro* activity was shown using the number of area value of treatment with vestaine A1 (5.0 μM) as a base of 100. Data is representative of three independent experiments. Each value is represented as the mean ± range ($n=2$ wells per group) A full colour version of this figure is available at the *Journal of Antibiotics* journal online.

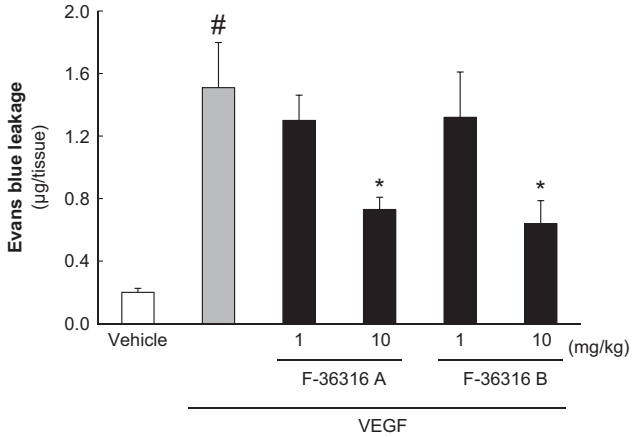

Figure 6 *In vivo* vascular leakage assays of F-36316 A and F-36316 B. The difference between vehicle and VEGF control was compared using a Student's t-test ($^{\#}P<0.05$). Statistically significant differences were determined by a Dunnett's multiple comparison test vs. VEGF control ($^{*}P<0.05$). Each value is represented as the mean ± s.e.m ($n=6$ per group).

dephosphorylation transition state of PTP.[21–23] Namely, this indicates that the phosphate group is mimicked by the tetronic anion of RK-682. If the tetronic acid moiety of F-36316 A could work like the phosphate group of S1P, F-36316 A might be a mimic of S1P and behave as an agonist to $S1P_1$. Indeed, F-36316 A shows a weak $S1P_1$ agonist activity (data not shown).

In this study, we discovered F-36316s as novel vasoactive compounds. However, it is necessary to investigate further whether F-36316s act as PTP inhibitors, $S1P_1$ agonists, or cause totally different effects. Identification of target molecule of these compounds might be useful to promote understanding of the complex mechanisms of angiogenesis or vessel stabilization.

EXPERIMENTAL PROCEDURES

Producing organism

The strain SANK 10414 was isolated from a minute fruit body collected in Shizuoka Pref., Japan. The ITS-5.8S rDNA sequence was determined via the method described by Hosoya *et al.*[24] The ITS-5.8S rDNA sequences of the strains that belong to the genus *Incrucipulum* and related species were obtained from the DDBJ database (http://www.ddbj.nig.ac.jp/)[24] and the MEGA program (version 6.05, http://www.megasoftware.net/) was used to draw the phylogenetic tree. The DDBJ/GenBank/EMBL accession number for the ITS-5.8S rDNA sequence of SANK 10414 is LC177543.

Fermentation

The growth of *Incrucipulum* sp. SANK 10414 on an agar slant was homogenized with sterilized water (5 ml). The homogenate (1 to 2 ml) was transferred into a 100-ml Erlenmeyer flask containing 30 ml of sterilized primary seed medium composed of soluble starch 2.0%, glucose 3.0%, glycerol 3.0%, soybean meal 1.0%, yeast extract 0.25%, gelatin 0.25%, NH_4NO_3 0.25%, agar 0.3% and Disfoam CB-442 (NOF, Tokyo, Japan) 0.005%. The flask was incubated at 23 °C for 7 days on a rotary shaker at 210 r.p.m. The primary seed culture (4 to 5 ml) was transferred into a 500-ml Erlenmeyer flask containing 80 ml of sterilized production medium, which was composed of maltose 2.0%, glucose 1.0%, cellulose powder 0.5%, Polypepton (Nihon Pharmaceutical, Tokyo, Japan) 0.2%, yeast extract 0.08%, KH_2PO_4 0.05%, $MgSO_4{\cdot}7H_2O$ 0.1%, $CaCl_2$ 0.0055%, $FeCl_3{\cdot}6H_2O$ 0.001%, $ZnSO_4{\cdot}7H_2O$ 0.0002% and Disfoam CB-442 0.005%. The flask was incubated at 23 °C for 14 days on a rotary shaker at 210 r.p.m.

General experimental procedures

IR spectra were obtained on an FT/IR-6100typeA spectrometer (JASCO Corp., Tokyo, Japan). UV spectra were recorded on a UV-265FW spectrometer (Shimadzu Corp., Kyoto, Japan). NMR spectra were recorded on AVC500 spectrometers equipped with DCH and TCI cryogenic probes (Bruker Corp., Billerica, MA, USA). High-resolution mass spectra were recorded on an LTQ Orbitrap XL spectrometer (Thermo Fisher Scientific, Inc., Waltham, MA, USA).

F-36316 A (just after dissolved in DMSO-d_6)

^{1}H NMR (500 MHz, DMSO-d_6, tetramethylsilane): δ_H 0.85 (3H, t, 7.0 Hz), 1.20–1.30 (20 H, overlapped), 1.42 (2H, m), 2.58 (2H, m), 4.20 (1H, br.), 4.38 (1H, br.). ^{13}C NMR (125 MHz, DMSO-d_6, TMS): δ_c 13.8, 22.0, 24.5, 28.6, 28.9, 29.0–29.1 (6 carbons), 31.2, 39.37 and 39.40 (tautomers)* 70.37 and 70.41 (tautomers), 80.5 and 80.6 (tautomers), 96.0 and 96.1 (tautomers), 171.9 and 172.0 (tautomers), 174.5 and 174.6 (tautomers), 192.2 and 192.3 (tautomers), 193.6 and 193.8 (tautomers). *These signals were measured by DEPT135 spectrum because they were not observed due to the overlap with DMSO-d_6 signals in ^{13}C NMR spectrum.

VS-G assay

The VS-G assay is a phenotype assay method using a co-culture system of GFP-labeled HUVECs with fibroblasts. In brief, GFP-HUVECs were seeded at 7.5×10^3 cells per well of 96-well plate onto the confluent fibroblasts' feeder layers in HuMedia-EG2. After adhesion of GFP-HUVECs to the fibroblasts' layers, test compounds in an assay medium (M199, 0.5% fetal calf serum) were added, and incubated at 37 °C for 3 days. Cell images were captured by using an In Cell Analyzer 6000 (GE healthcare Japan, Tokyo, Japan) or ImageXpress ULTRA (Molecular Devices, Sunnyvale, CA, USA). The value of area covered by GFP-HUVECs was analyzed using IN Cell Investigator 1.6 (GE healthcare Japan, Tokyo, Japan) or MetaXpress (Molecular Devices, Sunnyvale, CA, USA) and its value was used as the *in vitro* activity. Details of the assay method will be described in another report.[6] EC_{50} values of the F-36316A and B were shown using the number of area value of treatment with that of the vestaine A_1 (5.0 μM) as a base of 100.

In vivo vascular leakage assay

All experimental procedures were performed in accordance with the in-house guidelines of the Institutional Animal Care and Use Committee of Daiichi Sankyo Co., Ltd. The test compounds were soluble with 10% dimethyl sulfoxide (DMSO) in saline. Six- to 7-week-old C57/BL6 mice were injected i.p. with saline or test compounds. After 4 h, 100 μl of 1.5% Evans Blue was injected into their jugular veins. As soon as the mice were anesthetized with isoflurane inhalation, VEGF (60 ng per ear) was administrated intradermally into ears and circulated for 30 min. The mice were killed by CO_2 inhalation and their ears were removed. The Evans Blue was extracted in DMSO and its amount was measured at 650 nm with a SpectraMax M5 (Molecular Devices). Details of the assay method will be described in another report.[6] The mice injected with saline were used as vehicle and the mice injected with VEGF were used as VEGF control. *In vivo* activity was calculated as shown below.

Inhibition Activity (%) = 100−100 × [(Test compound)−(Vehicle)]/[(VEGF control)−(Vehicle)].

CONFLICT OF INTEREST

The authors declare no conflict of interest.

ACKNOWLEDGEMENTS

We are grateful to Dr Toshio Takatsu, Dr Yasunori Muramatsu and Mr Satoru Ohsuki for useful advice.

1 Bates, D. O. Vascular endothelial growth factors and vascular permeability. *Cardiovasc. Res.* **87**, 262–271 (2010).
2 Aiello, L. P. *et al.* Vascular endothelial growth factor in ocular fluid of patients with diabetic retinopathy and other retinal disorders. *N. Engl. J. Med.* **331**, 1480–1487 (1994).

3 Mathews, M. K., Merges, C., McLeod, D. S. & Lutty, G. A. Vascular endothelial growth factor and vascular permeability changes in human diabetic retinopathy. *Invest. Ophthalmol. Vis. Sci.* **38**, 2729–2741 (1997).
4 Weinberg, D. G. *et al.* Moyamoya disease: a review of histopathology, biochemistry, and genetics. *Neurosurg. Focus* **30**, E20 (2011).
5 Jain, R. K. Normalization of tumor vasculature: an emerging concept in antiangiogenic therapy. *Science* **307**, 58–62 (2005).
6 Ishimoto, Y. *et al.* A novel natural product-derived compound, vestaine A_1, exerts both pro-angiogenic and anti-permeability activity via a different pathway from VEGF. *Cell Physiol. Biochem.* **39**, 1905–1918 (2016).
7 Hirota-Takahata, Y. *et al.* Vestaines, novel vasoactive compounds, isolated from *Streptomyces* sp. SANK 63697. *J. Antibiot.* **70**, 179–186 (2017).
8 Yamaguchi, T., Saito, K., Tsujimoto, T. & Yuki, H. Nmr spectroscopic studies on the tautomerism in tenuazonic acid analogs. *J. Heterocyclic Chem.* **13**, 533–537 (1976).
9 Roggo, E. B. *et al.* 3-Alkanoyl-5-hydroxymethyl tetronic acid homologues and resistomycin: new inhibitors of HIV-1 protease I. Fermentation, isolation and biological activity. *J. Antibiot.* **47**, 136–142 (1994).
10 Roggo, E. B., Hug, P., Moss, S., Raschdorf, F. & Peter, H. H. 3-Alkanoyl-5-hydroxymethyl tetronic acid homologues: new inhibitors of HIV-1 protease II. Structure determination. *J. Antibiot.* **47**, 143–147 (1994).
11 Shoji, J. *et al.* Isolation and characterization of agglomerins A, B, C and D. *J. Antibiot.* **42**, 1729–1733 (1989).
12 Terui, Y. *et al.* Structures of agglomerins. *J. Antibiot.* **43**, 1245–1253 (1990).
13 Angawi, R. E. *et al.* Lowdenic acid: a new antifungal polyketide-derived metabolite from a new fungicolous *Verticillium* sp. *J. Nat. Prod.* **66**, 1259–1262 (2003).
14 Hamaguchi, T., Sudo, T. & Osada, H. RK-682, a potent inhibitor of tyrosine phosphatase, arrested the mammalian cell cycle progression at G1 phase. *FEBS Lett.* **372**, 54–58 (1995).
15 Sodeoka, M. *et al.* Asymmetric synthesis of a 3-acyltetronic acid derivative, RK-682, and formation of its calcium salt during silica gel column chromatography. *Chem. Pharm. Bull.* **49**, 206–212 (2001).
16 Goel, S. *et al.* Effects of vascular-endothelial protein tyrosine phosphate inhibition on breast cancer vasculature and metastatic progression. *J. Natl Cancer Inst.* **105**, 1188–1201 (2013).
17 Shen, J. *et al.* Targeting VE-PTP activates TIE2 and stabilizes the ocular vasculature. *J. Clin. Invest.* **124**, 4564–4576 (2014).
18 An, S., Zheng, Y. & Bleu, T. Sphingosine 1-phosphate-induced cell proliferation, survival, and related signaling events mediated by G protein-coupled receptors Edg3 and Edg5. *J. Biol. Chem.* **275**, 288–296 (2000).
19 Kimura, T. *et al.* Sphingosine 1-phosphate stimulates proliferation and migration of human endothelial cells possibly through the lipid receptors, Edg-1 and Edg-3. *Biochem. J.* **348**, 71–76 (2000).
20 Sammani, S. *et al.* Differential effects of sphingosine 1-phosphate receptors on airway and vascular barrier function in the murine lung. *Am. J. Respir. Cell Mol. Biol.* **43**, 394–402 (2010).
21 Sodeoka, M. *et al.* Synthesis of a tetronic acid library focused on inhibitors of tyrosine and dial-specificity protein phosphatases and its evaluation regarding VHR and cdc25B inhibition. *J. Med. Chem.* **44**, 3216–3222 (2001).
22 Usui, T. *et al.* Design and synthesis of a dimeric derivative of RK-682 with increased inhibitory activity against VHR, a dual-specificity ERK phosphatase: implications for the molecular mechanism of the inhibition. *Chem. Biol.* **8**, 1209–1220 (2001).
23 Hirai, G. & Sodeoka, M. Focused library with a core structure extracted from natural products and modified: application to phosphatase inhibitors and several biochemical findings. *Acc. Chem. Res.* **48**, 1464–1473 (2015).
24 Hosoya, T. *et al.* Molecular phylogenetic studies of *Lachnum* and its allies based on the Japanese material. *Mycosciense* **51**, 170–181 (2010).

Supplementary Information accompanies the paper on The Journal of Antibiotics website (http://www.nature.com/ja)